Adsorption 9: 133–142, 2003
© 2003 Kluwer Academic Publishers. *Manufactured in The Netherlands*.

Use of Nonlinear Frequency Response for Discriminating Adsorption Kinetics Mechanisms Resulting with Bimodal Characteristic Functions

MENKA PETKOVSKA*
Department of Chemical Engineering, Faculty of Technology and Metallurgy, University of Belgrade, Karnegijeva 4, 11000 Belgrade, Yugoslavia

LJUBICA T. PETKOVSKA
Department of Physical Chemistry, Vinča Institute of Nuclear Sciences, P.O.B. 522, 11001 Belgrade, Yugoslavia

Received April 29, 2002; Revised November 25, 2002; Accepted February 19, 2003

Abstract. One of the characteristic examples of the inability of the classical linear frequency response (FR) method to identify the correct kinetic mechanism is adsorption of some substances (*p*-xylene, 2-butane, propane or *n*-hexane) on silicalite-1. The linear FR resulted with bimodal FR characteristic functions, which fitted equally well to three different kinetic models: nonisothermal micropore diffusion, two independent isothermal diffusion processes, and an isothermal diffusion-rearrangement process. We show that the second order frequency response functions (FRFs), obtained from the nonlinear FR, can be used for discrimination among these three mechanisms. Starting from the nonlinear models, we derive the theoretical expressions for the first and second order FRFs corresponding to these three mechanisms and show that different shapes of the second order FRFs are obtained for each mechanism. This would enable identification of the real mechanism from nonlinear FR data.

Keywords: nonlinear mathematical models, nonlinear frequency response method, bimodal characteristic functions, isothermal and nonisothermal models

Introduction

Frequency response (FR) is one of the most commonly used methods for process dynamics investigation and model identification. After the pioneer work of Naphtali and Polinski (1963), it has also been used to investigate the kinetics of adsorption. A detailed list of references on investigation of adsorption kinetics by the FR method is given in some of our previous papers (Petkovska and Do, 1998, 2000). All those investigations assume system linearity, in spite the fact that adsorption systems are generally nonlinear.

One of the main drawbacks of this classical, linear frequency response method for investigation of adsorption kinetics is that, in a number of cases, same shapes of linear FR characteristic functions are obtained for different kinetic mechanisms, so the FR method is reduced to estimation of kinetic parameters of an assumed model. One example of such behaviour are the same shapes of characteristic curves obtained for adsorption governed by Langmuir kinetics, micropore diffusion or pore-surface diffusion mechanisms (Park et al., 1998). Another very characteristic example are the bimodal characteristic functions, with two maxima of the out-of-phase functions and two inflection points of the in-phase characteristic functions, obtained by Rees and co-workers, for adsorption of 2-butane, *p*-xylene, propane or *n*-hexane on silicalite-1 (Shen and Rees, 1991, 1995; Song and Rees, 1996, 1997). Their results were shown to fit equally well to three different mechanisms: nonisothermal micropore diffusion, two parallel isothermal diffusion processes,

*To whom correspondence should be addressed.

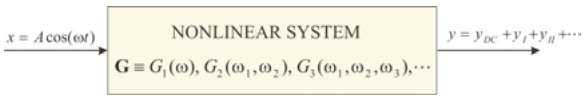

Figure 1. Frequency response of a nonlinear system.

and the so-called, isothermal diffusion-rearrangement process (Sun and Bourdin, 1993; Shen and Rees, 1995; Song and Rees, 1996, 1997).

In our work on investigation of adsorption kinetics by FR, we have been developing a new technique, based on nonlinear FR and on the concept of higher order frequency response functions (FRFs) (Petkovska and Do, 1998, 2000; Petkovska, 1999, 2000, 2001). Some details about nonlinear FR and the concept of higher order FRFs can be found in these references. Here we give only some basic remarks. Contrary to linear FR, which consists only of the basic (first) harmonic, nonlinear FR also contains a DC component and an indefinite number of higher harmonics (Fig. 1, Eq. (1)).

$$\begin{aligned} y &= y_{\mathrm{DC}} + y_{\mathrm{I}} + y_{\mathrm{II}} + y_{\mathrm{III}} + \cdots \\ &= y_{\mathrm{DC}} + B_{\mathrm{I}} \cos(\omega t + \varphi_{\mathrm{I}}) + B_{\mathrm{II}} \cos(2\omega t + \varphi_{\mathrm{II}}) \\ &\quad + B_{\mathrm{III}} \cos(3\omega t + \varphi_{\mathrm{III}}) + \cdots \end{aligned} \tag{1}$$

The concept of higher order FRFs assumes replacement of the nonlinear model **G** with a series of linear FRFs of the first, second, third, etc. order (G_1, G_2, G_3, etc.) (Weiner and Spina, 1980). For weakly nonlinear systems (such as adsorption ones) $G_1(\omega)$ corresponds to the dominant term of the first harmonic:

$$\begin{aligned} y_{\mathrm{I}} = B_{\mathrm{I}} \cos(\omega t + \varphi_{\mathrm{I}}) &= \{(A/2)G_1(\omega) \\ &\quad + 3(A/2)^3 G_3(\omega, \omega, -\omega) + \cdots\} e^{j\omega t} \\ &\quad + \{(A/2)G_1(-\omega) + 3(A/2)^3 \\ &\quad \times G_3(\omega, -\omega, -\omega) + \cdots\} e^{-j\omega t} \end{aligned} \tag{2}$$

$G_2(\omega,\omega)$ to the dominant term of the second harmonic:

$$\begin{aligned} y_{\mathrm{II}} = B_{\mathrm{II}} \cos(2\omega t + \varphi_{\mathrm{II}}) &= \{(A/2)^2 G_2(\omega, \omega) \\ &\quad + 4(A/2)^4 G_4(\omega, \omega, \omega, -\omega) + \cdots\} e^{2j\omega t} \\ &\quad + \{(A/2)^2 G_2(-\omega, -\omega) \\ &\quad + 4(A/2)^4 G_4(\omega, -\omega, -\omega, -\omega) + \cdots\} e^{-2j\omega t} \end{aligned} \tag{3}$$

$G_2(\omega, -\omega)$ to the dominant term of the DC component

$$\begin{aligned} y_{\mathrm{DC}} &= 2(A/2)^2 G_2(\omega, -\omega) \\ &\quad + 6(A/2)^4 G_4(\omega, \omega, -\omega, -\omega) + \cdots \end{aligned} \tag{4}$$

etc.

In our previous papers (Petkovska, 1999, 2000; Petkovska and Do, 2000) we have shown that the second order FRFs give enough information for discrimination among different single mechanisms of adsorption, owing to the difference in their shapes. The purpose of this paper is to show that different shapes of the theoretical second order FRFs are obtained for the three models used to describe bimodal characteristic curves obtained by Rees and his co-workers. That would enable identification of the correct kinetic mechanism, once having nonlinear FR experimental data.

We want to point out that our aim in this paper is not to analyse all cases which can result with bimodal FR characteristic curves, but only to show that the nonlinear FR method can efficiently resolve the dilemma about the correct mechanism corresponding to the experimental results of Rees and his co-workers.

Mathematical Models

The three models used to explain the bimodal characteristic curves have been given in detail elsewhere (Shen and Rees, 1991; Jordi and Do, 1992; Sun and Bourdin, 1993). Here we will give only the basic information about them and the model equations. In order to investigate nonlinear FR, we will use model versions with general nonlinear adsorption equilibrium relations. Model equations for the three models are listed in Table 1.

Model 1. This model assumes an isothermal mechanism of *two parallel, independent diffusion processes* in two different types of micropores (an assumption based on the presence of two types of channels: straight and sinusoidal, in silicalite-1) (Shen and Rees, 1991). The processes in the two types of pores are each defined by their separate diffusion coefficients (regarded as constants) and adsorption isotherm relations. The nonlinear adsorption isotherms are shown in the Taylor series form, and equilibrium at the micropore mouth is assumed. The model equations are given in the first row of Table 1 (Eqs. (5) to (9)). In these equations t is time, r_μ spatial coordinate of the microparticle and R_μ its half-dimension. All dependent variables: the gas pressure p, the sorbate concentration in the solid phase at position $r_\mu\, q$, and its mean value $\langle q \rangle$ are defined as nondimensional deviations from their steady state values. D_μ is the micropore diffusion coefficient, σ the shape factor (0 for slab, 1 for cylindrical and 2 for spherical microparticles) and χ the fraction of the

Table 1. Model equations.

Model	Model equations
Model 1:	Mass balances:
Two independent isothermal micropore diffusion processes	$\frac{\partial q_1}{\partial t} = D_{\mu_1}\nabla^2 q_1$ (5)
	$\frac{\partial q_2}{\partial t} = D_{\mu_2}\nabla^2 q_2$ (6)
	Boundary conditions:
	$r_\mu = 0$: $\frac{\partial q_1}{\partial r_\mu} = \frac{\partial q_2}{\partial r_\mu} = 0$ (7)
	$r_\mu = R_\mu$: $q_1 = f_1(p) = a_{p_1} p + b_{pp_1} p^2 + \cdots$
	$q_2 = f_2(p) = a_{p_2} p + b_{pp_2} p^2 + \cdots$ (8)
	Mean sorbate concentration in the particle:
	$\langle q \rangle = \chi \frac{\sigma+1}{R_\mu^\sigma} \int_0^{R_\mu} r_\mu^\sigma q_1(r_\mu)\, dr_\mu + (1-\chi)\frac{\sigma+1}{R_\mu^\sigma} \int_0^{R_\mu} r_\mu^\sigma q_2(r_\mu)\, dr_\mu$ (9)
Model 2:	Mass balances:
Isothermal diffusion-rearrangement model	$\frac{\partial q_1}{\partial t} + \delta \frac{\partial q_2}{\partial t} = D_{\mu_1}\nabla^2 q_1$ (10)
	$\frac{\partial q_2}{\partial t} = k_1(q_1+1)(q_{0_2} - q_2) - k_2(q_2+1)(q_{0_1} - q_1) = K_1 q_1 - K_2 q_2 + K_3 q_1 q_2$ (11)
	Boundary conditions:
	$r_\mu = 0$: $\frac{\partial q_1}{\partial r_\mu} = 0$ (12)
	$r_\mu = R_\mu$: $q_1 = f_1(p) = a_{p_1} p + b_{pp_2} p^2 + \cdots$ (13)
	Mean sorbate concentration in the particle: same as for Model 1
Model 3:	Material balance:
Nonisothermal micropore diffusion model	$\frac{\partial q}{\partial t} = D_\mu \nabla^2 q$ (14)
	Boundary conditions:
	$r_\mu = 0$: $\frac{\partial q}{\partial r_\mu} = 0$ (15)
	$r_\mu = R_\mu$: $q = f(p, T_p) = a_p p + a_T T_p + b_{pp} p^2 + b_{TT} T_p^2 + b_{pT} p T_p + \cdots$ (16)
	Mean sorbate concentration in the particle:
	$\langle q \rangle = \frac{\sigma+1}{R_\mu^\sigma} \int_0^{R_\mu} r_\mu^\sigma q(r_\mu) dr_\mu$ (17)
	Heat balance:
	$\frac{dT_p}{dt} = \xi \frac{d\langle q \rangle}{dt} + \zeta(T_g - T_p)$ (18)

sorbate corresponding to the micropores of the first type, at equilibrium. The subscripts 1 and 2 correspond to the pores of the first and second type, respectively. When the diffusion coefficients in the two types of micropores differ enough, the bimodal characteristic curves are obtained.

Model 2. This, so-called *isothermal diffusion-rearrangement* model (Jordi and Do, 1992), again corresponds to adsorbent with two types of micropores, but it assumes that diffusion takes place only in one type of micropores (transport pores), while the other type serves only for storage of the sorbed molecules (storage pores). This mechanisms can also result with bimodal characteristic curves. The model Eqs. (10) to (13) are given in the second row of Table 2. The rate of mass exchange between the two pore types is defined by a Langmuir rate Eq. (11). In these equations q_0 is the sorbate concentration in the micropores at maximal coverage, k_1 and k_2 the rate constants defining the mass transfer between the transport and the storage pores, χ the fraction of the sorbate corresponding to the

transport pores, at equilibrium, and δ the ratio of the equilibrium sorbate concentrations in the storage and in the transport pores. The subscripts 1 and 2 correspond to the transport and storage pores, respectively. All other notations are the same as for model 1. The assumption of the equilibrium at the micropore mouth, constant diffusivity and the Taylor series expansion expression of the adsorption isotherm are used as well.

Model 3. This model, which assumes that the adsorption kinetics is governed by a *single nonisothermal micropore diffusion process* (Sun and Bourdin, 1993), can also result with bimodal characteristic curves. The model Eqs. (14) to (18) are listed in the third raw of Table 1. The heat balance Eq. (18) was based on an assumption of a gas film heat transfer control with uniform particle temperature. In these equations T_p and T_g are the particle and gas temperatures, respectively, defined as nondimensional deviations from their steady state values, while ξ and ζ are the modified heat of adsorption and the modified heat transfer coefficient. All the other symbols, as well as the assumptions of constant diffusivity and equilibrium at the micropore mouth are used in the same way as for models 1 and 2. The adsorption equilibrium relation is again given in the Taylor series form, only this time taking into account both pressure and temperature dependence. A detailed description of this model, for the more general

Table 2. First and second order frequency response functions for three models (for $\sigma = 0$).

Model	Frequency response functions
Model 1:	First order FRF:
Two independent isothermal micropore diffusion processes	$F_{1,p}(\omega) = \chi a_{p_1}\Phi(\alpha_1(\omega)) + (1-\chi)a_{p_2}\Phi(\alpha_2(\omega))$ (19)
	Second order FRFs:
	$F_{2,pp}(\omega,\omega) = \chi b_{pp_1}\Phi(2\alpha_1(\omega)) + (1-\chi)b_{pp_2}\Phi(2\alpha_2(\omega))$ (20)
	$F_{2,pp}(\omega,-\omega) = \chi b_{pp_1} + (1-\chi)b_{pp_2}$ (21)
	with: $\Phi(\alpha(\omega)) = \dfrac{\tanh(\alpha)}{\alpha(\omega)}$, $\alpha_1(\omega) = \sqrt{\dfrac{j\omega}{D_{\mu_1}}}R_\mu$, $\alpha_2(\omega) = \sqrt{\dfrac{j\omega}{D_{\mu_2}}}R_\mu$
Model 2:	First order FRF:
Isothermal diffusion-rearrangement model	$F_{1,p}(\omega) = (\chi + (1-\chi)\beta(\omega))a_{p_i}\Phi(\alpha(\omega))$ (22)
	Second order FRFs:
	$F_{2,pp}(\omega,\omega) = (\chi + (1-\chi)\beta(2\omega))\{C^*\Phi(\alpha(2\omega)) + D_1^*\Phi(\alpha(\omega)) + D_2^*\cosh^{-2}(\alpha(\omega))\}$ $+ 0.5(1-\chi)K_1^{-1}K_3a_{p_1}^2\beta(\omega)\beta(2\omega)\{\Phi(\alpha(\omega)) + \cosh^{-2}(\alpha(\omega))\}$ (23)
	$F_{2,pp}(\omega,-\omega) = (\chi + (1-\chi)K_1K_2^{-1})b_{pp_1}$ $+ K_2^{-1}K_3a_{p_1}^2\ \mathrm{Re}(\beta(\omega))\{\alpha^2(\omega) - \bar{\alpha}^2(\omega)\}^{-1}\{\alpha(\omega)\Phi(\alpha(\omega)) - \bar{\alpha}(\omega)\Phi(\bar{\alpha}(\omega))\}$ (24)
	with: $\beta(\omega) = \dfrac{K_1}{K_2 + j\omega}$, $\alpha(\omega) = \sqrt{\dfrac{j\omega}{D_{\mu_1}}(1+\delta\beta(\omega))}R_\mu$, $\bar{\alpha}(\omega) = \mathrm{conj}(\alpha(\omega))$
	$D_1^* = \dfrac{K_3\delta a_{p_1}^2\beta(\omega)\beta(2\omega)\omega j}{K_1D_{\mu_1}(4\alpha^2(\omega) - \alpha^2(2\omega))}$, $D_2^* = -\dfrac{K_3\delta a_{p_1}^2\beta(\omega)\beta(2\omega)\omega j}{K_1D_{\mu_1}\alpha^2(2\omega)}$
	$C^* = b_{pp_1} - 2D_1^* + (D_1^* - D_2^*)\cosh^{-2}(2\alpha(\omega))$
	$\Phi(\alpha(\omega))$ same as for Model 1
Model 3:	First oder FRF:
Nonisothermal micropore diffusion model	$F_{1,p}(\omega) = \dfrac{a_p\Phi(\alpha(\omega))}{1 - a_T\Lambda(\omega)\Phi(\alpha(\omega))}$ (25)
	Second order FRFs:
	$F_{2,pp}(\omega,\omega) = \dfrac{b_{pp} + b_{pT}\Lambda(\omega)F_{1,p}(\omega) + b_{TT}\Lambda^2(\omega)F_{1,p}^2(\omega)}{1 - a_T\Lambda(2\omega)\Phi(\alpha(2\omega))}\Phi(\alpha(2\omega))$ (26)
	$F_{2,pp}(\omega,-\omega) = b_{pp} + b_{pT}Re(\Lambda(\omega)F_{1,p}(\omega)) + b_{TT}\lvert\Lambda(\omega)F_{1,p}(\omega)\rvert^2$ (27)
	with: $\Lambda(\omega) = \dfrac{\xi\omega j}{\varsigma + j\omega}$, $\alpha(\omega) = \sqrt{\dfrac{j\omega}{D_\mu}}R_\mu$,
	$\Phi(\alpha(\omega))$ same as for Model 1

case of variable diffusivity, can be found in Petkovska (2000).

First and Second Order FRFs

Starting from the nonlinear models defined in Table 1, the first and higher order FRFs can be derived. As they are derived from the models defined on the particle level, these are particle FRFs (Petkovska, 2001), relating the change of the mean sorbate concentration in the microparticle $\langle q \rangle$ and the change of the gas pressure p. The procedure for theoretical derivation of higher order FRFs is given in detail in one of our previous papers (Petkovska, 2001). The same notation as in our previous papers was used to designate these functions ($F_{1,p}$, $F_{2,pp}$,...). It was found that the second order FRFs give enough information for model discrimination (Petkovska and Do, 2000), so our analysis is restricted to the first and second order FRFs. For slab microparticle geometry (which can be assumed for silicalite-1 (Shen and Rees, 1997)), the first and second order FRFs can be derived analytically. The resulting expressions are listed in Table 2.

Although model 3 is nonisothermal, and thus requires six series of particle FRFs for complete description of the system (Petkovska, 2000, 2001), only the FRFs correlating the mean concentration in the solid phase $\langle q \rangle$ and the gas pressure p are given, in order to be compared with the functions obtained for models 1 and 2 which are isothermal.

Using the expressions given in Table 2, the first and second order FRFs corresponding to the three models were simulated. Some of the simulated results are given in Figs. 2–4 (corresponding to models 1–3, respectively). The model parameters for these simulations, given in Table 3, correspond to adsorption of n-hexane on silicalite-1 at 0.133 kPa (1 Torr) and 373 K (Shen and Rees, 1997).

The FRFs are complex functions of frequency. In order to get full insight into all their features, we are

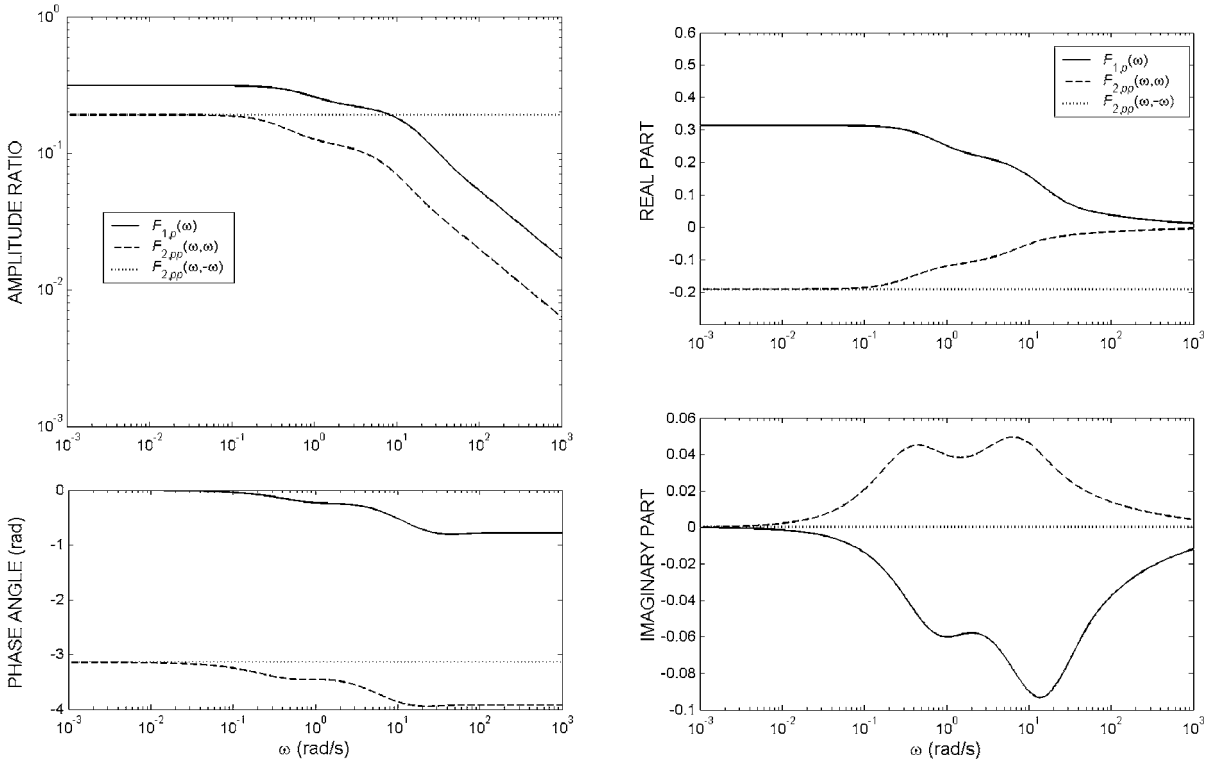

(a) (b)

Figure 2. First and second order FRFs for model 1 (for n-hexane on silicalite-1 at 0.133 kPa and 373 K): (a) amplitude and phase functions; (b) real and imaginary parts.

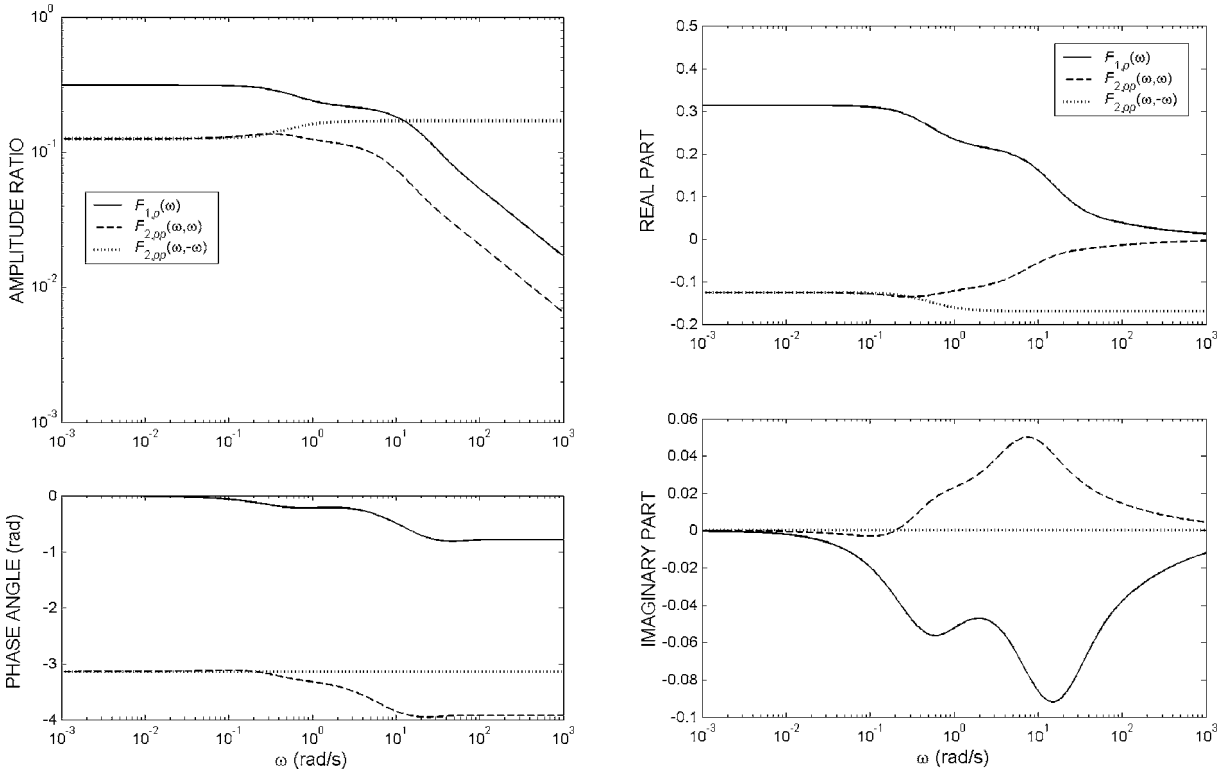

Figure 3. First and second order FRFs for model 2 (for *n*-hexane on silicalite-1 at 0.133 kPa and 373 K): (a) amplitude and phase functions; (b) real and imaginary parts.

showing them in two different forms: amplitude ratios and phase angles vs. frequency (Figs. 2(a)–4(a)) and real and imaginary parts vs. frequency (Figs. 2(b)–4(b)).

The results presented in these figures are only a segment of the simulation results, obtained with the model parameters given in Table 3. Here is the summary of the characteristic features of the first and second order FRFs for the three models:

- *Model 1*: The functions $F_{1,p}(\omega)$ and $F_{2,pp}(\omega, \omega)$ have similar behaviour: amplitude functions have horizontal asymptotes for $\omega \to 0$ and asymptotes with slope -0.5 for $\omega \to \infty$, with two changes of slope; phase functions go from 0 or $-\pi$ (for $\omega \to 0$) to $-\pi/4$ or $-5\pi/4$ (for $\omega \to \infty$), with two inflection points; the real parts have two changes of slope with horizontal plateaus; the imaginary parts have two minima ($F_{1,p}(\omega)$) or two maximums ($F_{2,pp}(\omega, \omega)$).

  The function $F_{2,pp}(\omega, -\omega)$ is constant, real and, for the case of favourable isotherms, negative (Petkovska, 2000):

$$F_{2,pp}(\omega, -\omega) = \chi b_{pp1} + (1 - \chi) b_{pp2} \qquad (28)$$

- *Model 2*: The first order FRF $F_{1,p}(\omega)$ has same characteristics as for model 1.

  The second order FRF $F_{2,pp}(\omega, \omega)$ has similar asymptotic behaviour as $F_{1,p}(\omega)$. For the case presented in Fig. 3 it has a small maximum of the amplitude characteristic and a small minimum of the real part, and its imaginary part changes the sign. In some simulations for other steady-state pressures and temperatures, imaginary parts with two maximums were also obtained.

  The second order FRF $F_{2,pp}(\omega, -\omega)$ has horizontal asymptotes at different levels for $\omega \to 0$ and $\omega \to \infty$:

$$\lim_{\omega \to 0} F_{2,pp}(\omega, -\omega) = \left(\chi + (1 - \chi) K_1 K_2^{-1}\right) b_{pp_1} + (1 - \chi) K_1 K_2^{-2} K_3 a_{p_1}^2 \qquad (29)$$

Table 3. Model parameters used for simulation—adsorption of *n*-hexane on silicalite-1 at 0.133 kPa (1 Torr) and 373 K (Shen and Rees, 1997).

Model 1	Model 2	Model 3
$D_{\mu 1} = 2.3322 \times 10^{-9}$ m^2/s	$D_{\mu 1} = 2.4083 \times 10^{-9}$ m^2/s	$D_{\mu} = 2.6878 \times 10^{-9}$m^2/s
$D_{\mu 2} = 1.2407 \times 10^{-10}$ m^2/s	$R_{\mu} = 2 \times 10^{-5}$ m	$R_{\mu} = 2 \times 10^{-5}$ m
$R_{\mu} = 2 \times 10^{-5}$ m	$K_1 = 0.2085$	$a_p = 0.3274$
$a_{p1} = 0.51454$	$K_2 = 0.5236$	$a_T = -1.1054$
$b_{pp1} = -0.24979$	$K_3 = 0.5436$	$b_{pp} = -0.22021$
$a_{p2} = 0.19344$	$a_{p1} = 0.45675$	$b_{TT} = 0.46125$
$b_{pp2} = -0.15602$	$b_{pp1} = -0.24813$	$b_{pT} = 0.38156$
$\chi = 0.37574$	$\chi = 0.47953$	$\xi = 0.37092$
	$\delta = 1.0854$	$\zeta = 0.70423$ s^{-1}

$$\lim_{\omega \to \infty} F_{2,pp}(\omega, -\omega) = \left(\chi + (1-\chi) K_1 K_2^{-1}\right) b_{pp_1} \tag{30}$$

so its amplitude is an increasing, and its real part a decreasing function of frequency.

- *Model 3*: $F_{1,p}(\omega)$ has same characteristics as for models 1 and 2.

The second order FRF $F_{2,pp}(\omega, \omega)$ has similar asymptotic behaviour as $F_{1,p}(\omega)$. For the case presented in Fig. 4, its characteristic curves have similar

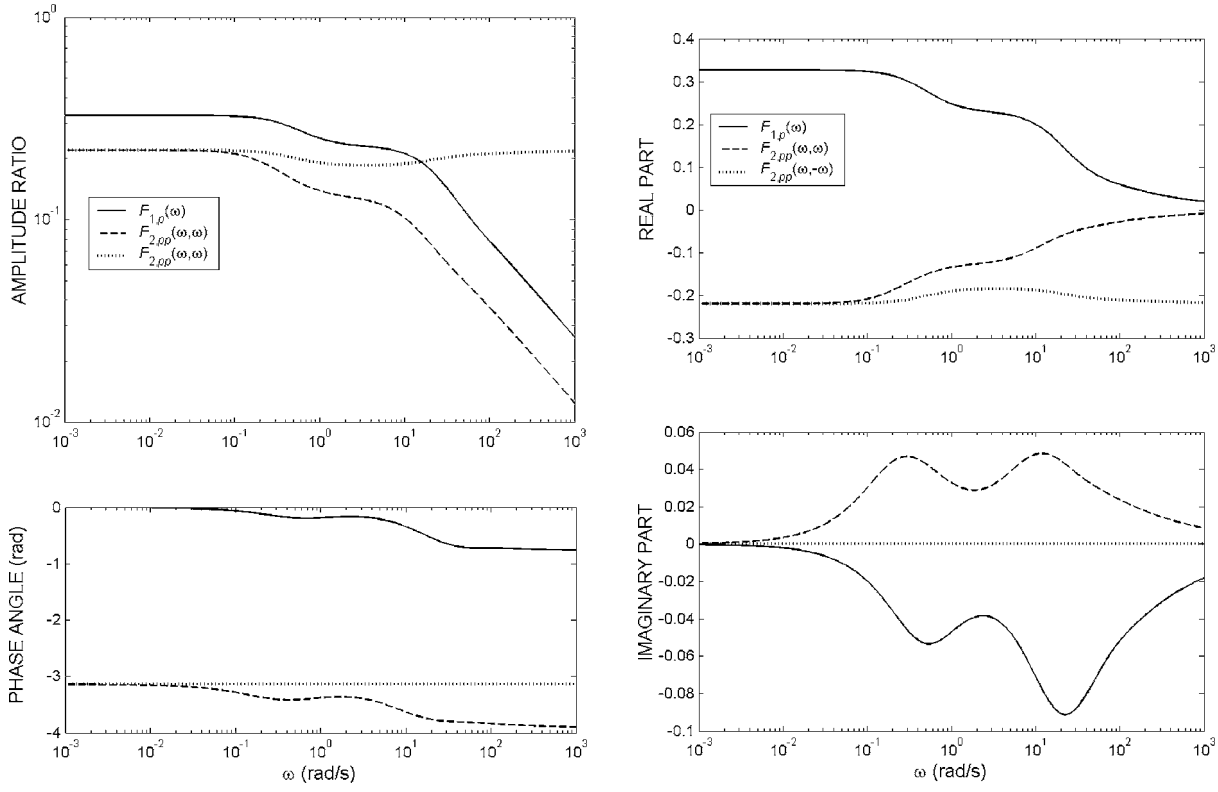

(a) (b)

Figure 4. First and second order FRFs for model 3 (for *n*-hexane on silicalite-1 at 0.133 kPa and 373 K): (a) amplitude and phase functions; (b) real and imaginary parts.

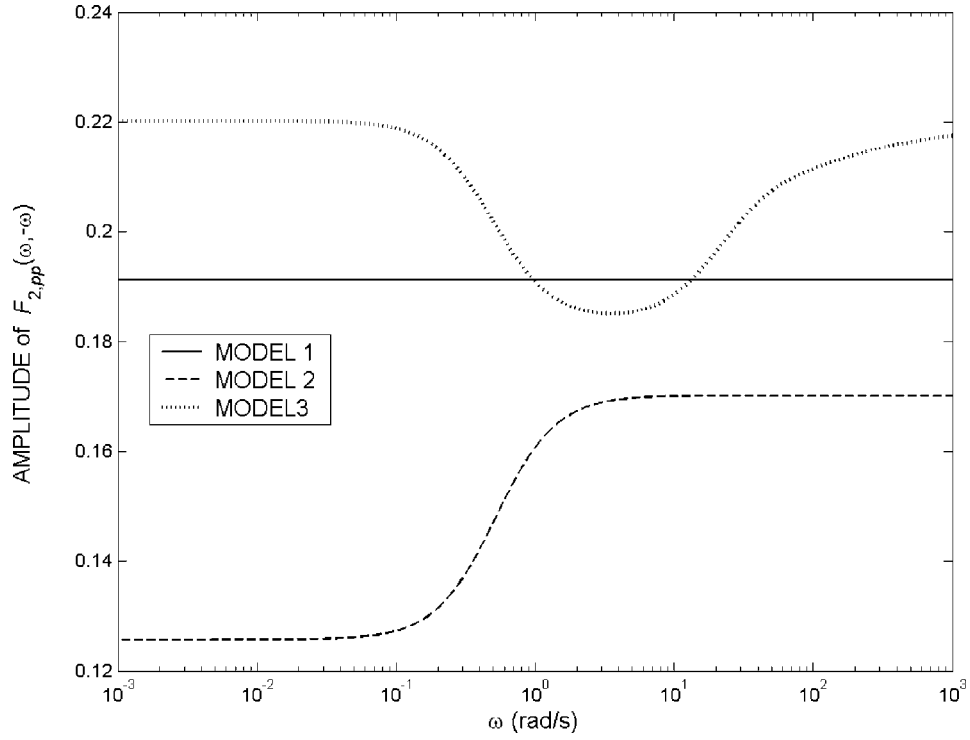

Figure 5. Amplitude functions of $F_{2,pp}(\omega, -\omega)$ for models 1–3.

shapes as $F_{1,p}(\omega)$, just of the opposite sign. For some other cases, a maximum of the amplitude characteristic and a minimum of the real part, with a change of sign of the imaginary part were obtained (Petkovska, 2000).

The second order FRF $F_{2,pp}(\omega, -\omega)$ has horizontal asymptotes for $\omega \to 0$ and $\omega \to \infty$ at the same level:

$$\lim_{\omega \to 0} F_{2,pp}(\omega, -\omega) = \lim_{\omega \to \infty} F_{2,pp}(\omega, -\omega) = b_{pp} \tag{31}$$

but shows a minimum of the amplitude characteristic and a maximum of the real part, for the case shown in Fig. 4. For some other cases, the amplitude characteristics had a maximum and the real parts a minimum (Petkovska, 2000).

Conclusions

The analysis of the second order particle FRFs corresponding to the three models used to explain bimodal FR curves shows that they have some specific features that can be used for their discrimination. The function $F_{2,pp}(\omega, -\omega)$, which defines the main term of the DC component of the nonlinear FR, seems especially interesting in that sense: it is constant for the case of two independent isothermal micropore diffusion processes, its amplitude increases between two horizontal asymptotes for the isothermal diffusion-rearrangement process and it has an extremum for the case of a single nonisothermal micropore diffusion process (the amplitudes of the $F_{2,pp}(\omega, -\omega)$ functions corresponding to the three models are presented together in Fig. 5, for comparison). This means that the second order FRF $F_{2,pp}(\omega, -\omega)$, or, practically, the DC component of the nonlinear FR, would give enough information for discrimination among the three models commonly used to explain the bimodal FR curves obtained with silicalite-1, and in that way for correct and unique identification of the kinetic mechanism governing the adsorption process. In a similar way, the nonlinear FR could be used for discrimination among different mechanisms suspected in reaction systems.

The three models analysed in this paper are not the only ones resulting with bimodal frequency response curves. They could also be obtained in a number of

other cases, when two or more kinetic mechanisms are influencing the overall rate of the process (e.g., micropore-macropore diffusion, micropore diffusion with finite mass transfer rate, etc.). But, these cases were not in the focus of this paper. The nonlinear frequency responses and the higher order FRFs of such systems will be analysed in one of our future papers.

Nomenclature

a_p	First order pressure coefficient in the Taylor expansion of the adsorption isotherm
a_T	First order temperature coefficient in the Taylor expansion of the adsorption isotherm
b_{pp}	Second order pressure coefficient in the Taylor expansion of the adsorption isotherm
b_{TT}	Second order temperature coefficient in the Taylor expansion of the adsorption isotherm
b_{pT}	Second order mixed coefficient in the Taylor expansion of the adsorption isotherm
D_μ	Micropore diffusion coefficient, $m^2\ s^{-1}$
$F_{1p}(\omega)$	First order particle $\langle q \rangle$ vs. p frequency response function
$F_{2pp}(\omega_1, \omega_2)$	Second order particle $\langle q \rangle$ vs. p frequency response function
k_1, k_2	Rate constants for mass transfer between transport and storage pores, s^{-1} (for model 2)
$K_1 = k_1 q_{02} + k_2$	Constant defined in Eq. (11), s^{-1}
$K_2 = k_2 q_{01} + k_1$	Constant defined in Eq. (11), s^{-1}
$K_3 = k_2 - k_1$	Constant defined in Eq. (11), s^{-1}
p	Gas pressure defined as nondimensional deviation from steady state
q	Sorbate concentration in the solid phase at position r_μ, defined as nondimensional deviation from steady state
q_0	Nondimensional sorbate concentration in the solid phase at maximal coverage
$\langle q \rangle$	Average sorbate concentration in the solid phase, defined as nondimensional deviation from steady state
r_μ	Spatial coordinate of the microparticle, m
R_μ	Particle half-dimension, m
t	Time, s
T_g	Gas temperature, defined as nondimensional deviation from steady state
T_p	Particle temperature, defined as nondimensional deviation from steady state

Greek Symbols

δ	Ratio of the equilibrium sorbate concentrations in the storage and in the transport pores (model 2)
χ	Fraction of sorbate corresponding to the micropores of the first type, for model 1, or to the transport pores, for model 2, at equilibrium
σ	Shape factor (0 for slab, 1 for cylindrical and 2 for spherical geometry)
ξ	Modified heat of adsorption
ζ	Modified heat transfer coefficient, s^{-1}

Subscripts

1	First type (model 1) or transport pores (model 2)
2	Second type (model 1) or storage pores (model 2)

Abbreviations

FR	Frequency response
FRF	Frequency response function

References

Jordi, R.G. and D.D. Do, "Analysis of the Frequency Response Method for Sorption in Zeolite Crystals with Finite Intracrystal Reversible Mass Exchange," *J. Chem. Soc. Faraday Trans.*, **88**, 2411 (1992).

Naphtali, L.M. and L.M.Polinski, "A Novel Technique for Characterization of Adsorption Rates On Heterogeneous Surfaces," *J. Physic. Chem.*, **67**, 369 (1963).

Park, I.S., M. Petkovska, and D.D. Do, "Frequency Response of an Adsorber with Modulation of the Inlet Molar Flow-Rate—I. A Semi-Batch Adsorber," *Chem. Eng. Sci.*, **53**, 819 (1998).

Petkovska, M., "Nonlinear Frequency Response of Isothermal Adsorption Controlled by Pore-Surface Diffusion," *Bul. Chem. Technol. Macedonia*, **18**, 149 (1999).

Petkovska, M., "Non-Linear Frequency Response of Non-Isothermal Adsorption Controlled by Micropore Diffusion with Variable Diffusivity," *J. Serb. Chem. Soc.*, **65**, 939 (2000).

Petkovska, M., "Nonlinear Frequency Response of Nonisothermal Adsorption Systems," *Nonlinear Dynamics*, **26**, 351 (2001).

Petkovska, M. and D.D. Do, "Nonlinear Frequency Response of Adsorption Systems: Isothermal Batch and Continuous Flow Adsorbers," *Chem. Eng. Sci.*, **53**, 3081 (1998).

Petkovska, M. and D.D. Do, "Use of Higher-Order Frequency Response Functions for Identification of Nonlinear Adsorption Kinetics: Single Mechanisms Under Isothermal Conditions," *Nonlinear Dynamics*, **21**, 353 (2000).

Shen, D.M. and L.V.C. Rees, "Adsorption and Diffusion of *n*-Butane and 2-Butane in Silicalite-1," *Zeolites*, **11**, 684 (1991).

Shen, D.M. and L.V.C. Rees, "Analysis of Bimodal Frequency-Response Behaviour of *p*-Xylene Diffusion in Silicalite-1," *J. Chem. Soc. Faraday Trans.*, **91**, 2027 (1995).

Song, L. and L.-V.C. Rees, "Frequency Response Diffusion of Propane in Silicalite-1," *Microporous Materials*, **6**, 363 (1996).

Song, L. and L.V.C. Rees, "Adsorption and Transport of *n*-Hexane in Silicalite-1 by Frequency Response Technique," *J. Chem. Soc. Faraday Trans.*, **93**, 649 (1997).

Sun, L.M. and V. Bourdin, "Measurement of Intrasrystalline Diffusion by the Frequency Response Method: Analysis and Interpretation of Bimodal Response Curves," *Chemical Engineering Science*, **48**, 3783 (1993).

Weiner, D.D. and J.F. Spina, "Sinusoidal Analysis and Modelling of Weakly Nonlinear Systems," Van Nostrand Reinhold, New York, 1980.